RADIO SCIENCE, VOL. 47, RS5006, doi:10.1029/2012RS005008, 2012

Evaluation of time domain electromagnetic fields radiated by constant velocity moving particles traveling along an arbitrarily shaped cross-section waveguide using frequency domain Green's functions

M. Jiménez Nogales,[1] S. Marini,[2] B. Gimeno Martínez,[3] A. Álvarez Melcón,[1] F. D. Quesada Pereira,[1] V. E. Boria Esbert,[4] P. Soto,[4] S. Cogollos,[4] and D. Raboso[5]

Received 2 March 2012; revised 15 June 2012; accepted 24 July 2012; published 21 September 2012.

[1] A technique for the accurate computation of the time domain electromagnetic fields radiated by a charged distribution traveling along an arbitrarily shaped waveguide region is presented. Based on the transformation (by means of the standard Fourier analysis) of the time-varying current density of the analyzed problem to the frequency domain, the resulting equivalent current is further convolved with the dyadic electric and magnetic Green's functions. Moreover, we show that only the evaluation of the transverse magnetic modes of the structure is required for the calculation of fields radiated by particles traveling in the axial direction. Finally, frequency domain electric and magnetic fields are transformed back to the time domain, just obtaining the total fields radiated by the charged distribution. Furthermore, we present a method for the computation of the wakefields of arbitrary cross-section uniform waveguides from the resulting field expressions. Several examples of charged particles moving in the axial direction of such waveguides are included.

Citation: Jiménez Nogales, M., S. Marini, B. Gimeno Martínez, A. Álvarez Melcón, F. D. Quesada Pereira, V. E. Boria Esbert, P. Soto, S. Cogollos, and D. Raboso (2012), Evaluation of time domain electromagnetic fields radiated by constant velocity moving particles traveling along an arbitrarily shaped cross-section waveguide using frequency domain Green's functions, *Radio Sci.*, *47*, RS5006, doi:10.1029/2012RS005008.

1. Introduction

[2] From radiotherapy to nuclear physics research, particle accelerators constitute a powerful device under continuous development. Actual applications of accelerators and storage rings introduce high restrictive design constraints on beam intensity and emittance [*Salah and Dolique*, 1999; *Salah*, 2004; *Gai et al.*, 1997]. In order to achieve optimum performance, an accurate understanding of the involved physics is required. In this sense, the evaluation of the fields radiated by a charged particle moving linearly at constant velocity within a beampipe is particularly important, since it may influence the motion of trailing particles [*Panofsky and Wenzel*, 1956; *Wangler*, 2008; *Zotter and Kheifets*, 1998]. In a particle accelerator, the beampipe is excited by an electromagnetic field during the accelerating stage to store and accelerate beams of charged particles. The particles are usually packed into bunches and launched at the appropriate time to take advantage of the accelerating phases, in order to achieve relativistic velocities [*Bane et al.*, 1985]. After the accelerating circuit, the velocity of a beam should remain constant; but the electromagnetic radiation of moving charges may influence the motion of other particles and bunches. The electromagnetic field created by a charge is scattered on the metallic walls of the waveguide and acts back on trailing charges, thus inducing energy loss, beam instabilities and some secondary effects like the heating of sensitive components [*Figueroa et al.*, 1988]. The interaction with the structure can be described by impedances in the frequency domain, or equivalently by wakefields in the time domain [*Yokoya*, 1993a; *Stupakov et al.*, 2007]. These parameters have to be taken into account during the design of an accelerator, as they restrict the choice of materials and shape of components [*Burov and Danilov*, 1999].

[3] The wakefields critically depend on the geometry of the structure [*Danilov*, 2000]. The radiation of particles within waveguides has deserved the attention of many researchers in different fields of the electromagnetic theory [*Rosing and Gai*, 1990; *Ng*, 1990; *Xiao et al.*, 2001; *Hess*

[1]Information and Signal Theory Department, Technical University of Cartagena, Cartagena, Spain.
[2]Departamento de Física, Ingenieria de Sistemas y Teoría de la Señal, Universidad de Alicante, San Vicente del Raspeig, Spain.
[3]Applied Physics Department (ICMUV), University of Valencia, Valencia, Spain.
[4]Communications Department-iTEAM, Technical University of Valencia, Valencia, Spain.
[5]European Space Agency, European Space Research and Technology Center, Noordwijk, Netherlands.

Corresponding author: F. D. Quesada Pereira, Information and Signal Theory Department, Technical University of Cartagena, Campus de la Muralla del Mar, Cuartel de Antigones, C. P. ES-30202, Cartagena, Spain. (fernando.quesada@upct.es)

0048-6604/12/2012RS005008

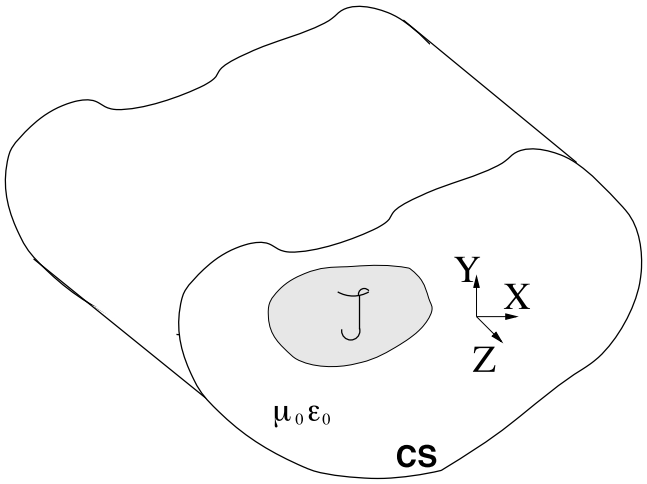

Figure 1. Schematic of an arbitrary charge distribution moving inside a uniform arbitrarily shaped cross-section waveguide region.

et al., 2007]. The solution of wakefields for rectangular and circular waveguides is well known [*Wangler*, 2008; *Zotter and Kheifets*, 1998; *Gluckstern et al.*, 1993]; moreover, in *Gluckstern et al.* [1993] a formula is given for the specific case of charges traveling on the symmetry axes within an elliptical guide. This formula has been extensively followed to estimate the wakefields in beampipes similar to the elliptical geometry [*Rumolo et al.*, 2001; *Zimmermann*, 1997]. The absence of analytical expressions for predicting the radiation within many geometries demands the development of numerical techniques for the analysis of arbitrary waveguides [*Kim et al.*, 1990; *Jing et al.*, 2003; *Lutman et al.*, 2008; *Zagorodnov*, 2006]. Usually, particle-in-cell codes are used to compute wakefields. In this article, we present an alternative full-wave modal method for the analysis of the electromagnetic radiation of charges in motion within uniform waveguides with arbitrary cross-section. The method here presented is based on the dyadic three-dimensional electric and magnetic Green's functions formulation in the frequency domain. The radiated fields are obtained from the convolution of the Green's functions with the current distribution of the bunch. Then, the fields are expressed in the time domain by means of the Fourier's Transform technique, from which the wakefields are finally derived. The effect of the velocity on beams has been traditionally omitted in the accelerators publications, where the ultrarelativistic approach is assumed [*Gluckstern et al.*, 1993; *Yokoya*, 1993b; *Kim et al.*, 1990; *Bane et al.*, 1985; *Rosing and Gai*, 1990; *Iriso-Ariz et al.*, 2003; *Lutman et al.*, 2008; *Palumbo et al.*, 1984]. In this sense, the present work represents a contribution since different velocities for the particles can be used in the proposed formulation. The presented formulation is completely analytic except in the calculation of the modes of the waveguide, which must be numerically computed. This fact reduces significantly the associated error of the method to the accuracy of the numerical technique used for the modal analysis of the structure. Moreover, the proposed formulation can treat waveguides of arbitrary shapes, what makes it a suitable method when non-canonical geometries are considered. In this sense, this method gives a practical contribution, since many modern accelerating structures are based on non-canonical waveguides.

[4] The paper has been organized in three sections. In the next one, the theoretical formulation of the problem is detailed. This section is divided in three blocks, corresponding to the dyadic electric and magnetic Green's functions, the fields created by moving charged particles, and the resulting wakefields. Afterwards, some examples of charges moving lengthwise within arbitrary waveguides are tackled by the presented derivation. Finally, conclusions are outlined.

2. Theory

2.1. Basic Formulation

[5] The type of geometry analyzed in this paper consists of an arbitrary cross-section homogeneous waveguide that is uniform along the direction of propagation, which coincides with the z axis (see Figure 1). Losses are not considered, and the guide is filled with vacuum, ε_0 being the electric permittivity of free space and μ_0 the magnetic permeability of free space; speed of light is given by $c = 1/\sqrt{\mu_0 \varepsilon_0}$. In this context, the vector position is divided in its transverse and axial components, $\mathbf{r} = \mathbf{r}_t + z\hat{\mathbf{z}}$. For this uniform cross-section waveguide region, it is well known that the solutions of Maxwell equations in the frequency domain can be expressed in terms of TE and TM modes [*Conciauro et al.*, 2000; *Collin*, 1991; *Felsen and Marcuvitz*, 1994; *Jackson*, 1999]. The transverse electric and magnetic fields can be decomposed into an infinite set of waveguide modes:

$$\mathbf{E}_t(\mathbf{r},\omega) = \sum_m V_m(z,\omega)\mathbf{e}_m(\mathbf{r}_t) \tag{1a}$$

$$\mathbf{H}_t(\mathbf{r},\omega) = \sum_m I_m(z,\omega)\mathbf{h}_m(\mathbf{r}_t) \tag{1b}$$

where V_m and I_m are the voltage and current modal amplitudes, and $\mathbf{e}_m$ and $\mathbf{h}_m$ are the electric and magnetic normalized vector modal functions, respectively. The normalization condition satisfied by these functions is given by

$$\int_{CS} \mathbf{e}_m \cdot \mathbf{e}_n dS = \int_{CS} \mathbf{h}_m \cdot \mathbf{h}_n dS = \delta_{m,n} \tag{2}$$

where CS is the waveguide cross-section, and $\delta_{m,n}$ is the Kronecker delta function. On the other hand, the axial components are expressed in terms of the scalar potentials Φ_m [*Felsen and Marcuvitz*, 1994]:

$$E_z(\mathbf{r},\omega) = \frac{1}{i\omega\varepsilon_0}\sum_m I_m^{TM}(z,\omega)k_{t_m}^2\Phi_m^{TM}(\mathbf{r}_t) \tag{3a}$$

$$H_z(\mathbf{r},\omega) = \frac{1}{i\omega\mu_0}\sum_m V_m^{TE}(z,\omega)k_{t_m}^2\Phi_m^{TE}(\mathbf{r}_t) \tag{3b}$$

i being the imaginary unit $i = \sqrt{-1}$; k_{t_m} are the modal transverse wave numbers, and the frequency is $f = \frac{\omega}{2\pi}$. A time-harmonic dependence $e^{i\omega t}$ is assumed and omitted throughout this paper. The modal characteristic impedances are given by $Z_m^{TE} = (\omega\mu_0)/k_{z_m}$ and $Z_m^{TM} = k_{z_m}/(\omega\varepsilon_0)$; k_{z_m} being the propagation factor in the axial direction. The dispersion

relationship satisfied by these modes is $k^2 = k_{t_m}^2 + k_{z_m}^2$, where $k = \omega\sqrt{\mu_0\varepsilon_0}$ is the free space wave number. An exponential factor of the form $\exp(-ik_{z_m}z)$ is assumed inside the modal amplitudes $V(z)$ and $I(z)$, for waves traveling in the positive z-direction.

[6] In our problem we have a time-varying arbitrarily shaped charged distribution radiating inside a waveguide region, as depicted in Figure 1, which is described by its volumetric charge density $\rho(\mathbf{r}, t)$ as well as its current density $\mathcal{J}(\mathbf{r}, t) = \rho(\mathbf{r}, t)\,\mathbf{v}(\mathbf{r}, t)$, where $\mathbf{v}$ is the velocity vector; note that both densities are also related through the continuity equation [*Jackson*, 1999]. In our formulation, the first step relies on the evaluation of the Fourier transform of the time domain current density,

$$\mathbf{J}(\mathbf{r}, \omega) = \int_{-\infty}^{+\infty} \mathcal{J}(\mathbf{r}, t) e^{-i\omega t} dt \tag{4}$$

$\mathbf{J}$ being the frequency domain current density. The next step consists on the evaluation of the frequency domain electric and magnetic fields radiated by such harmonic currents, which will be performed by means of the following volume integrals:

$$\mathbf{E}(\mathbf{r}, \omega) = \int_V \overline{\mathbf{G}}_e(\mathbf{r}, \mathbf{r}', \omega) \cdot \mathbf{J}(\mathbf{r}', \omega) dV' \tag{5a}$$

$$\mathbf{H}(\mathbf{r}, \omega) = \int_V \overline{\mathbf{G}}_m(\mathbf{r}, \mathbf{r}', \omega) \cdot \mathbf{J}(\mathbf{r}', \omega) dV' \tag{5b}$$

where $\overline{\mathbf{G}}_e$ and $\overline{\mathbf{G}}_m$ are the frequency domain three-dimensional dyadic electric and magnetic Green's functions of the infinite waveguide region, respectively. The evaluation of Green's functions is a classical problem of electromagnetics, which has been extensively treated in the technical literature [*Collin*, 1991; *Felsen and Marcuvitz*, 1994; *Tai*, 1993; *Hanson and Yakovlev*, 2002]. The dyadic Green's functions of an infinite uniform cross-section waveguide represents the electric and magnetic fields radiated by a time-harmonic unit impulse current source placed at an arbitrary location given by the vector position $\mathbf{r}'$. The source element can be oriented along any direction, thus allowing to solve three-dimensional current problems. In the spectral domain, the dyadic electric and magnetic Green's functions are expressed in terms of the normalized electric and magnetic TE and TM vector modal functions, as follows [*Felsen and Marcuvitz*, 1994; *Wang*, 1978; *Rahmat-Samii*, 1975; *Deshpande*, 1997]

$$\begin{aligned}
\overline{\mathbf{G}}_e(\mathbf{r}, \mathbf{r}', \omega) = &-\frac{1}{2}\sum_m Z_m^{TM} \mathbf{e}_m^{TM}(\mathbf{r}_t)\mathbf{e}_m^{TM}(\mathbf{r}_t')e^{-ik_{z_m}|z-z'|} \\
&-\frac{1}{2}\sum_m Z_m^{TE} \mathbf{e}_m^{TE}(\mathbf{r}_t)\mathbf{e}_m^{TE}(\mathbf{r}_t')e^{-ik_{z_m}|z-z'|} \\
&-\frac{u(z-z')}{i2\omega\varepsilon_0}\sum_m k_{t_m}^2 \Phi_m^{TM}(\mathbf{r}_t)\hat{\mathbf{z}}\mathbf{e}_m^{TM}(\mathbf{r}_t')e^{-ik_{z_m}|z-z'|} \\
&+\frac{u(z-z')}{i2\omega\varepsilon_0}\sum_m k_{t_m}^2 \mathbf{e}_m^{TM}(\mathbf{r}_t)\hat{\mathbf{z}}\Phi_m^{TM}(\mathbf{r}_t')e^{-ik_{z_m}|z-z'|} \\
&-\frac{1}{2\omega^2\varepsilon_0^2}\sum_m \frac{k_{t_m}^4}{Z_m^{TM}} \Phi_m^{TM}(\mathbf{r}_t)\Phi_m^{TM}(\mathbf{r}_t')\hat{\mathbf{z}}\hat{\mathbf{z}}e^{-ik_{z_m}|z-z'|} \\
&-\frac{\delta(\mathbf{r}-\mathbf{r}')}{i\omega\varepsilon_0}\hat{\mathbf{z}}\hat{\mathbf{z}}
\end{aligned} \tag{6a}$$

$$\begin{aligned}
\overline{\mathbf{G}}_m(\mathbf{r}, \mathbf{r}', \omega) = &-\frac{u(z-z')}{2}\sum_m \mathbf{h}_m^{TM}(\mathbf{r}_t)\mathbf{e}_m^{TM}(\mathbf{r}_t')e^{-ik_{z_m}|z-z'|} \\
&-\frac{u(z-z')}{2}\sum_m \mathbf{h}_m^{TE}(\mathbf{r}_t)\mathbf{e}_m^{TE}(\mathbf{r}_t')e^{-ik_{z_m}|z-z'|} \\
&-\frac{1}{i2\omega\mu_0}\sum_m Z_m^{TE} k_{t_m}^2 \Phi_m^{TE}(\mathbf{r}_t)\hat{\mathbf{z}}\mathbf{e}_m^{TE}(\mathbf{r}_t')e^{-ik_{z_m}|z-z'|} \\
&+\frac{1}{i2\omega\mu_0}\sum_m \frac{k_{t_m}^2}{Z_m^{TM}} \mathbf{h}_m^{TM}(\mathbf{r}_t)\hat{\mathbf{z}}\Phi_m^{TE}(\mathbf{r}_t')e^{-ik_{z_m}|z-z'|}
\end{aligned} \tag{6b}$$

where the sign function $u(z - z')$ and the Dirac delta function $\delta(\mathbf{r} - \mathbf{r}')$ have been introduced.

[7] Finally, we must derive the time domain electric and magnetic fields using the standard inverse Fourier transform,

$$\begin{Bmatrix} \mathcal{E}(\mathbf{r}, t) \\ \mathcal{H}(\mathbf{r}, t) \end{Bmatrix} = \frac{1}{2\pi}\int_{-\infty}^{+\infty} \begin{Bmatrix} \mathbf{E}(\mathbf{r}, \omega) \\ \mathbf{H}(\mathbf{r}, \omega) \end{Bmatrix} e^{i\omega t} d\omega \tag{7}$$

The present formulation is completely general, and now it will be applied to analyze several problems of radiation of charged particles. The presence of arbitrarily shaped cross-section waveguides will be considered in this work.

2.2. Study of the Fields Radiated by a Charged Particle Uniformly Moving in the Axial Direction

[8] A particle accelerator structure basically consists of a waveguide circuit alternating accelerating cavities and through-sections. The particles, packed in bunches, are injected into the structure and accelerated up to ultra-relativistic velocities by the action of the accelerating cavities which contain RF high-power electromagnetic fields. In the present section, the electromagnetic fields radiated by such particles within the beampipe of a particle accelerator or within a generic homogeneous waveguide are discussed. Since the particles velocity is unchanged between successive accelerating cavities, they can be reduced to the study of constant velocity particles traveling along an infinite homogeneous waveguide. There is a source particle carrying charge q uniformly moving in the z direction with constant velocity v; we assume that $v \geq 0$. The charge and current densities of this particle are represented in the time domain by

$$\rho(\mathbf{r}', t) = q\delta(x' - x_0)\delta(y' - y_0)\delta(z' - vt) \tag{8a}$$

$$\vec{\mathcal{J}}(\mathbf{r}', t) = \rho(\mathbf{r}', t)v\hat{\mathbf{z}} \tag{8b}$$

respectively. Thus, the Cartesian coordinates $\mathbf{r}_0 = (x_0, y_0)$ define the transverse position of the particle. Following the presented technique, now we have to calculate the frequency domain current density applying (4) to (8), easily obtaining

$$\mathbf{J}(\mathbf{r}', \omega) = q\delta(x' - x_0)\,\delta(y' - y_0)e^{-i\omega z'/v}\hat{\mathbf{z}} \tag{9}$$

Secondly, the frequency domain electric and magnetic fields can be analytically derived by inserting (9) into (5), thus obtaining

$$\mathbf{E}_t(\mathbf{r},\omega) = \frac{q}{v\varepsilon_0}\sum_m k_{t_m}^2 \mathbf{e}_m^{TM}(\mathbf{r}_t)\Phi_m^{TM}(\mathbf{r}_0)\frac{e^{-i\omega z/v}}{\left(\frac{\omega}{v\gamma}\right)^2 + k_{t_m}^2} \tag{10a}$$

$$E_z(\mathbf{r},\omega) = -\frac{iq}{\omega\varepsilon_0}\sum_m k_{t_m}^4 \Phi_m^{TM}(\mathbf{r}_t)\Phi_m^{TM}(\mathbf{r}_0)\frac{e^{-i\omega z/v}}{\left(\frac{\omega}{v\gamma}\right)^2 + k_{t_m}^2} \tag{10b}$$

$$\mathbf{H}_t(\mathbf{r},\omega) = q\sum_m k_{t_m}^2 \mathbf{h}_m^{TM}(\mathbf{r}_t)\Phi_m^{TM}(\mathbf{r}_0)\frac{e^{-i\omega z/v}}{\left(\frac{\omega}{v\gamma}\right)^2 + k_{t_m}^2} \tag{10c}$$

$$H_z(\mathbf{r},\omega) = 0 \tag{10d}$$

After applying the inverse Fourier transformation (7) to these expressions, we finally obtain the time domain fields radiated by the charged particle (see Appendix A for a deeper explanation of the inverse Fourier transformation),

$$\vec{\mathcal{E}}_t(\mathbf{r},t) = \frac{q\gamma}{2\varepsilon_0}\sum_m k_{t_m}\mathbf{e}_m^{TM}(\mathbf{r}_t)\Phi_m^{TM}(\mathbf{r}_0)e^{-k_{t_m}\gamma|vt-z|} \tag{11a}$$

$$\mathcal{E}_z(\mathbf{r},t) = -\frac{q}{2\varepsilon_0}u\left(t-\frac{z}{v}\right)\cdot\sum_m k_{t_m}^2\Phi_m^{TM}(\mathbf{r}_t)\Phi_m^{TM}(\mathbf{r}_0)e^{-k_{t_m}\gamma|vt-z|} \tag{11b}$$

$$\vec{\mathcal{H}}_t(\mathbf{r},t) = \frac{qv\gamma}{2}\sum_m k_{t_m}\mathbf{h}_m^{TM}(\mathbf{r}_t)\Phi_m^{TM}(\mathbf{r}_0)e^{-k_{t_m}\gamma|vt-z|} \tag{11c}$$

$$\mathcal{H}_z(\mathbf{r},t) = 0 \tag{11d}$$

where $\gamma \equiv 1/\sqrt{1-\beta^2}$ is the relativistic factor, $\beta \equiv v/c$ being the velocity in terms of the speed of light in vacuum. Note that only the TM modes are being excited. It should be observed that the magnetic field is zero for a static charge ($v = 0$). Due to the analytical nature of the method, it achieves good accuracy as compared to numerical techniques based on differential equations, such as finite differences or finite elements. This is because these techniques require the discretization of the whole volume, and the accuracy strongly depends on how fine the structure is discretized.

[9] It is worth to analyze these expressions in the case that the particle velocity approaches the speed of light limit (ultrarelativistic case). Then, the field power concentrates on a cross-plane moving together with the charge. The transverse components of the fields turn into a Dirac-delta, whereas the longitudinal field vanishes (see Appendix B for details):

$$\lim_{v\to c^-}\vec{\mathcal{E}}_t(\mathbf{r},t) = \frac{q}{2c\varepsilon_0}\delta\left(t-\frac{z}{c}\right)\sum_m \mathbf{e}_m^{TM}(\mathbf{r}_t)\Phi_m^{TM}(\mathbf{r}_0) \tag{12a}$$

$$\lim_{v\to c^-}\mathcal{E}_z(\mathbf{r},t) = 0 \tag{12b}$$

$$\lim_{v\to c^-}\vec{\mathcal{H}}_t(\mathbf{r},t) = \frac{q}{2}\delta\left(t-\frac{z}{c}\right)\sum_m \mathbf{h}_m^{TM}(\mathbf{r}_t)\Phi_m^{TM}(\mathbf{r}_0) \tag{12c}$$

$$\lim_{v\to c^-}\mathcal{H}_z(\mathbf{r},t) = 0. \tag{12d}$$

2.3. Study of the Wakefields

[10] The electromagnetic fields created by the particles in the previous section induce surface charges and currents in the walls of the beampipe, which act back on particles and beams traveling behind. The trajectory and the velocity of traveling particles are modified by the presence of such surface charges, thus resulting in bunch instabilities. It is a convention for relativistic electron beams to know these space forces as wakefields, although they also propagate in front of the source charge for $v < c$. The wakefield effect is analyzed in the frame of the actual work by means of the definition of a δ-function wake potential. This function characterizes the net impulse delivered from a unit-strength source charge to a trailing charge along an homogeneous waveguide section of length L. Both charges travel at the same velocity v along the same or parallel trajectories, spaced in the axial direction by a distance s (s can be greater or smaller than L). The δ-function wake potential has been defined as in section 11.3 of *Wangler* [2008], here adapted to particles with a velocity below the limit c and traveling within a lossless waveguide:

$$\mathbf{w}_t(\mathbf{r},\mathbf{r}',s) = \frac{1}{q}\int_0^L \vec{\mathcal{E}}_t\left(\mathbf{r},t=\frac{z+s}{v}\right)dz + \frac{v\mu_0}{q}\int_0^L \hat{z} \times \vec{\mathcal{H}}_t\left(\mathbf{r},t=\frac{z+s}{v}\right)dz \tag{13a}$$

$$w_z(\mathbf{r},\mathbf{r}',s) = -\frac{1}{q}\int_0^L \mathcal{E}_z\left(\mathbf{r},t=\frac{z+s}{v}\right)dz \tag{13b}$$

where w_z and $\mathbf{w}_t$ are the longitudinal and transverse δ-function wake potentials; $\mathbf{r}'$ and $\mathbf{r}$ stand for the initial position of the leading and the trailing charges, respectively. Applying these definitions to the field expressions (11), one obtains (see Appendix C):

$$\mathbf{w}_t(\mathbf{r},\mathbf{r}',s) = \frac{L}{2\gamma\varepsilon_0}\sum_m k_{t_m}\mathbf{e}_m^{TM}(\mathbf{r}_t)\Phi_m^{TM}(\mathbf{r}_t')e^{-k_{t_m}\gamma s} \tag{14a}$$

$$w_z(\mathbf{r},\mathbf{r}',s) = \frac{L}{2\varepsilon_0}\sum_m k_{t_m}^2\Phi_m^{TM}(\mathbf{r}_t)\Phi_m^{TM}(\mathbf{r}_t')e^{-k_{t_m}\gamma s} \tag{14b}$$

Note that last expressions are zero at the physical limit $v \to c^-$ for any separation between charges $s \neq 0$. It means that no wakefield is present in a lossless homogeneous waveguide for charges traveling at the speed of light. Wakefields appear as consequence of wall discontinuities, finite conductivity of the material and a velocity of charges less than the ultrarelativistic limit. The integrated effect over a finite distribution of charged particles is described by the wake potential. The wake potential of a complete bunch on a single charge

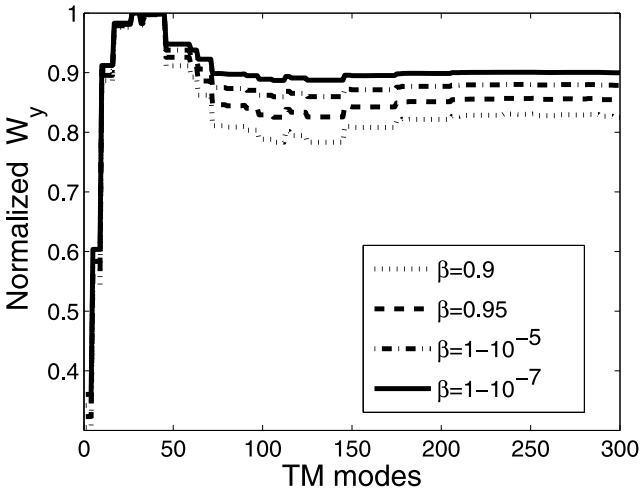

Figure 2. Influence of the number of modes used in the solution of the δ-function wake potential (14) for the waveguide geometry represented in Figure 3. Comparison between several charge velocities for a fixed distance s = 5 mm (the wake function has been normalized to make the comparison possible). Note that the number of modes necessary for the convergence of the solution reduces when the velocity increases; similar effect would produce an increment in the distance s.

can be determined by the convolution of the wake δ-function with the charge distribution of the bunch.

[11] The convergence of an expression in infinite series like (14) is dominated by the exponential part; the larger the exponent is, the faster the series converges to a realistic solution. This effect is shown in Figure 2, where the wake potential in a waveguide example is approached by different number of terms in the summation expression. The convergence of the series (14) is also guaranteed in the limit s approaches zero, as is demonstrated in *Álvarez Melcón and Mosig* [2000]. This limit represents the waveguide cross-plane that contains the source charge. In this case, the exponent in the series vanishes and the number of modes required for convergence is extremely high. Thus, it is more efficient to tackle the $s = 0$ problem by means of a numerical approaching method, such as to estimate the value of fields and wake-potentials from the solution of a series of decreasing distance points, or by using extrapolation techniques as in *Álvarez Melcón and Mosig* [1999].

3. Numerical Results

[12] Next, the presented formulation will be applied to the analysis of wakefields within structures of arbitrary geometry, thus proving the capabilities of this method. In a first example, a cross-shaped waveguide has been chosen for discussing the effect of rounding the corners of the inner waveguide walls. In the second example, several geometries are compared to a waveguide similar to the CERN Large Hadron Collider (LHC) beampipe.

3.1. Rounded-Corner Cross-Shaped Waveguides

[13] It is well known that the electromagnetic fields within a waveguide are particularly strong near convex wedges. The power focusing in these areas gives rise to undesirable consequences, like the heating of walls and the attraction of free particles. The accumulation of charged particles in a small region of the beampipe will produce changes in the resistivity of the component and multipactoring effects, both causing losses and defocusing in the beam. For this reason, sharp wedges are avoided in the design of accelerating structures as far as possible.

[14] With the aim of studying the influence of corners in the geometry of a beampipe, an homogeneous cross-shaped waveguide with rounded corners (see Figure 3) has been analyzed. Three different radii of curvature r for the corners of the waveguide are considered for comparison. The size of the arms of the cross has been selected to a = 3 mm. The wakefields for two different trajectories of a source particle are compared.

[15] For the calculation of the modal expansion of the waveguide, the two-dimensional Boundary Integral-Resonant Mode Expansion (BI-RME) method was used. The BI-RME method [*Conciauro et al.*, 1984, 2000] has been revealed as a robust and high computational efficient modal technique for the characterization of arbitrary waveguides, whose accuracy is discussed in *Conciauro et al.* [1984], *Cogollos et al.* [2003] and *Bozzi et al.* [2001]. The accuracy of the results shown in this example and in the next one is only dependent on the number of modes used in the summation expressions (11) and (14), and on the accuracy of the numerical computation of such modes. The BI-RME method here used allows to compute a large number of modes with high precision on a standard PC [*Conciauro et al.*, 1984; *Cogollos et al.*, 2003; *Bozzi et al.*, 2001]. A total of 450 electric *TM*-modal vectors were generated by a BI-RME based tool [*Cogollos et al.*, 2003] and used to evaluate the δ-function wake potential at any point.

[16] Figures 4 and 5 show the wake-potential distribution in the *XY*-plane at s = 5 μm behind the source. In Figure 4 the source particle is on the center of the waveguide and the normalized velocity is $\beta = 1 - 10^{-7}$; on the other hand, in Figure 5 the source is within one of the arms of the

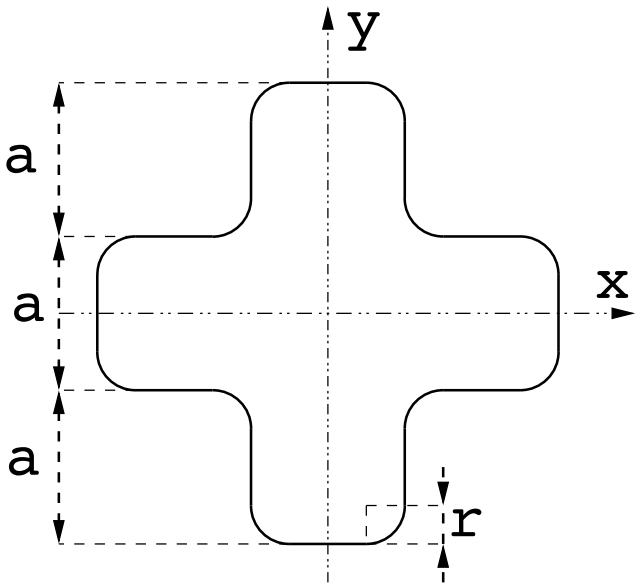

Figure 3. Cross-section of a rounded-corner cross-shaped waveguide.

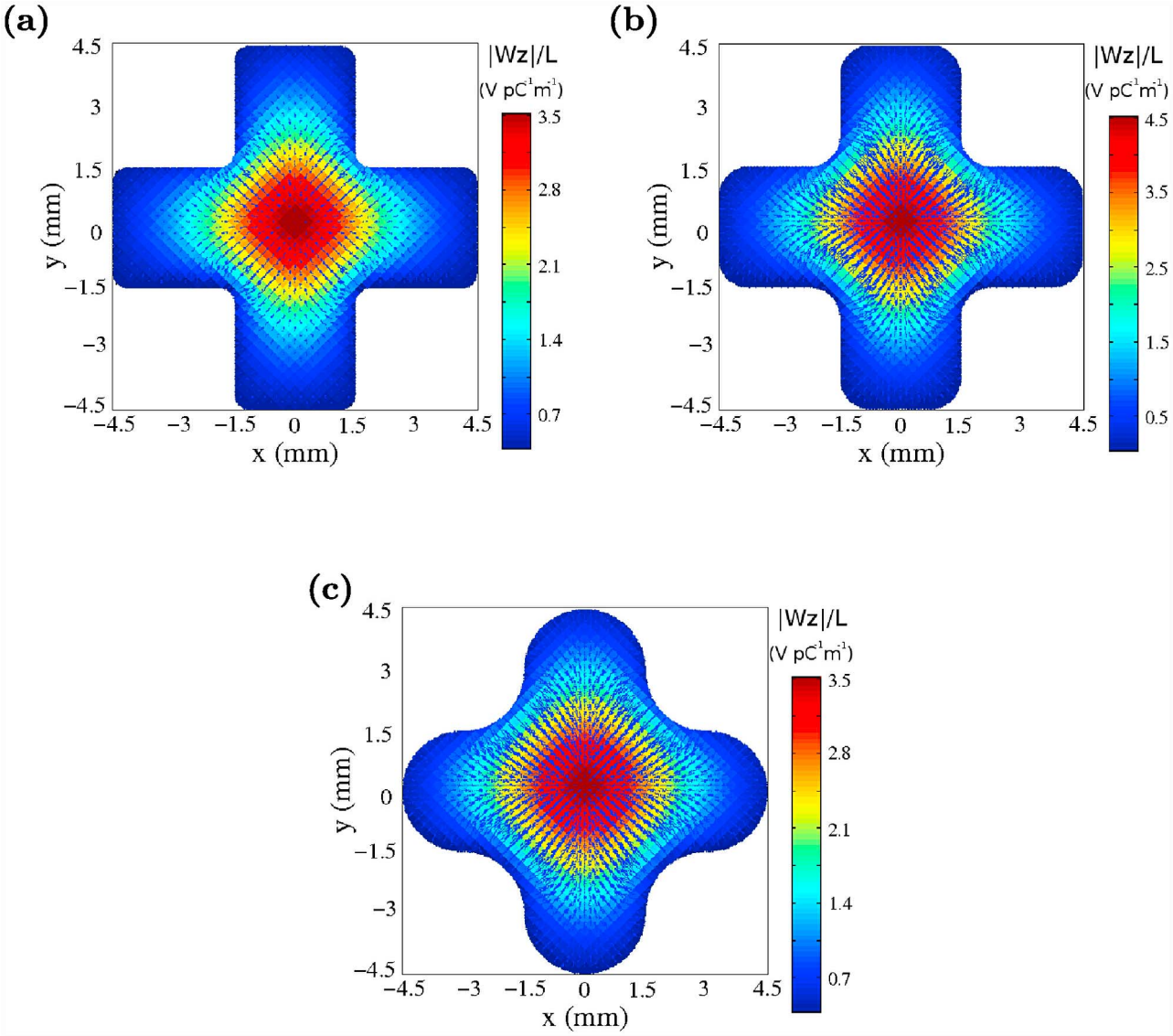

Figure 4. The δ-function wake potential for cross-shaped waveguides with different radii of curvature. Picture of the transverse plane at a distance $s = 5$ μm behind the source charge. $\mathbf{r}'_t = (0, 0)$, $\beta = 1 - 10^{-7}$. The colorbar stands for $|W_z|/L$ (V pC^{-1} m^{-1}) and the arrows point to the direction of $\mathbf{w}_t$. (a) $r = a/8$, (b) $r = a/4$, (c) $r = a/2$.

waveguide, and the normalized velocity is $\beta = 1 - 10^{-6}$. The CPU time used for the computation of a unique point is 42 seconds in a standard PC at 3.2 GHz.

[17] Cuts along the y-axis of preceding pictures are found in Figures 6 and 7, where w_x has been omitted (this component is null on the y-axis because of the symmetry of the problem). The maximum value for w_z varies with the radius of curvature, but obviously coincides with the source location, as can be seen in Figures 6b and 7b. The behavior of the transverse wake potential is different. From Figure 6a it is observed that, when the source is at the center, the maximum magnitude for w_y lays at a point within the interval $\pm(a/2, a/2 + r)$; this interval coincides with the narrowing of the waveguide at the beginning of one arm of the cross. On the other hand, when the source is shifted from the center (Figure 7a), the transverse wake potential has an offset related to the deviation of the leading charge.

[18] The different scales for the wake potential intensity shown in both trajectories can be explained by the difference in velocity. Note that the electric field distribution is contracted into a disk perpendicular to the direction of motion with a narrow angular spread of the order of $1/\gamma$, as reported in *Wangler* [2008]. In Figure 8, the wake potential is plotted for a testing and a trial charge depending on the velocity. It is shown that the intensity of the longitudinal wake potential decreases with the velocity as a consequence of the electric field contraction.

3.2. A Comparative Study of the Wake Potentials for Different Waveguide Geometries

[19] A homogeneous waveguide with a cross-section similar to the beampipe used in the CERN LHC Laboratory [*Iriso-Ariz et al.*, 2003] has been modeled by means of a BI-RME based tool. The wake potential in this structure is

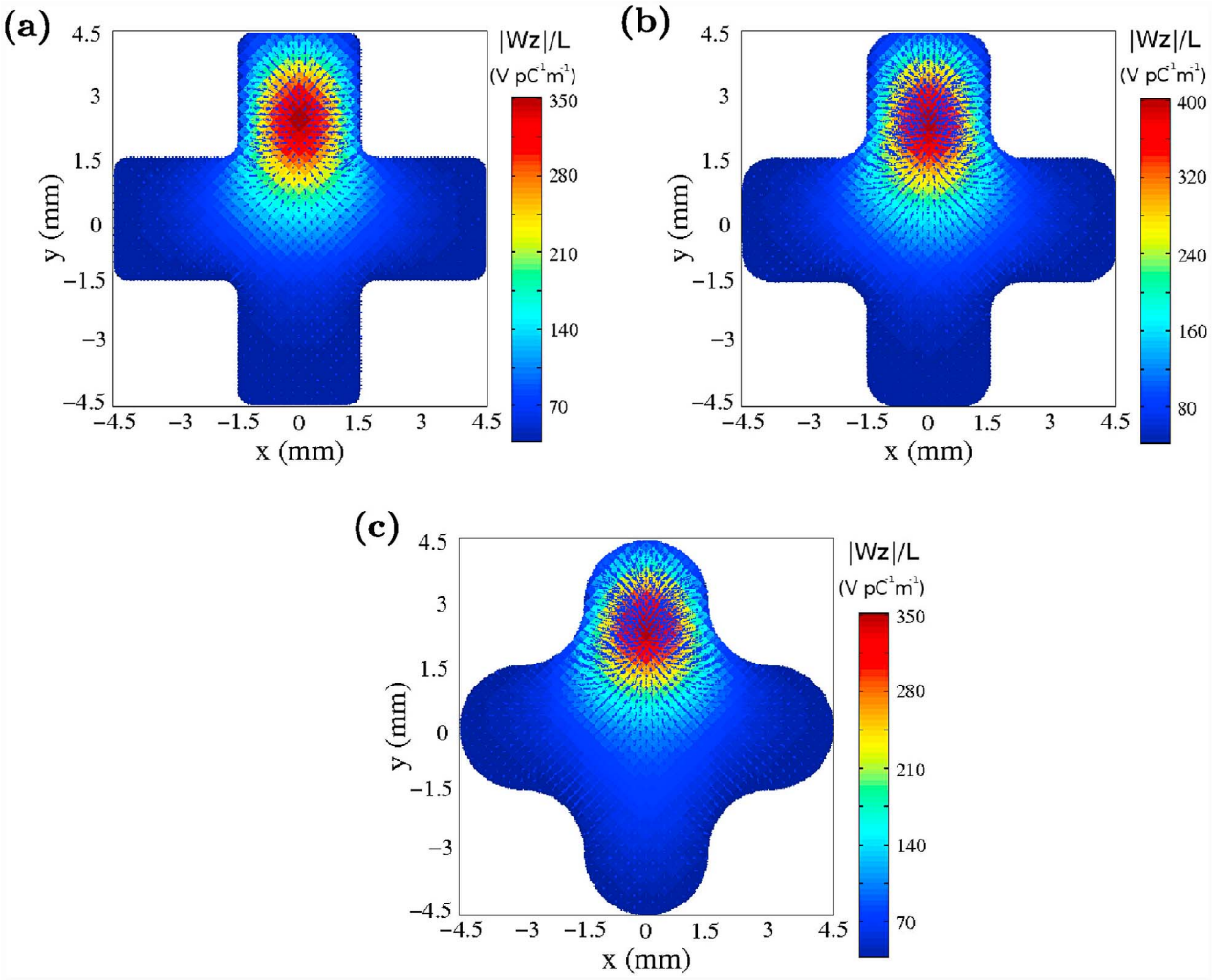

Figure 5. The δ-function wake potential for cross-shaped waveguides with different radii of curvature. Picture of the transverse plane at a distance $s = 5$ μm behind the source charge. $\mathbf{r}'_t = (0, 2.3)$ mm, $\beta = 1 - 10^{-6}$. The colorbar stands for $|W_z|/L$ (V pC^{-1} m^{-1}) and the arrows point to the direction of $\mathbf{w}_t$; (a) $r = a/8$, (b) $r = a/4$, (c) $r = a/2$.

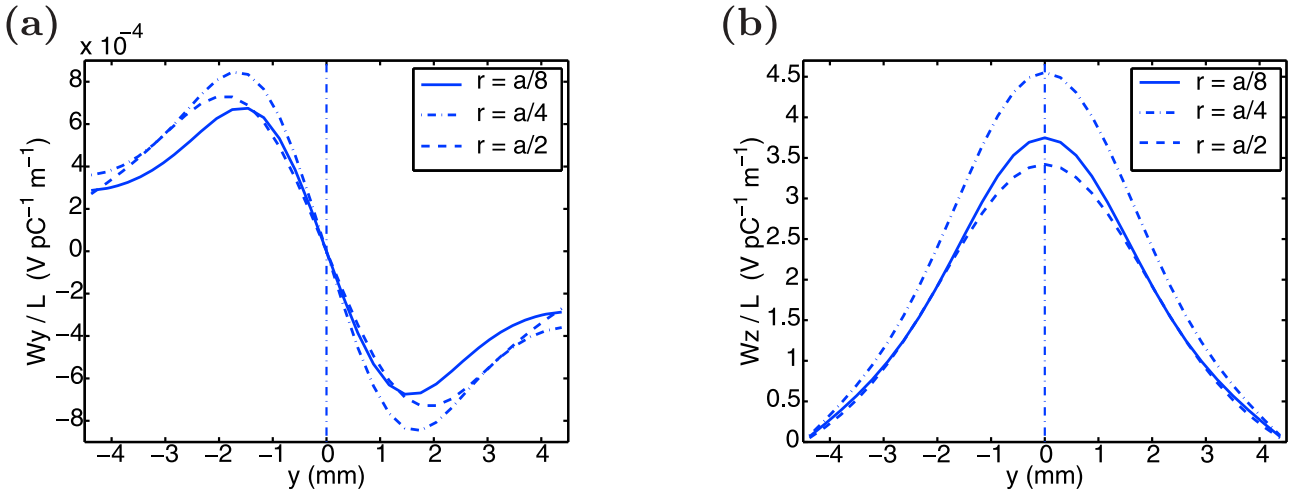

Figure 6. Dependence of the δ-function wake potential on the transverse position of a trailing charge along the y-axis for cross-shaped waveguides. The leading charge is located at the center of the waveguide (vertical dashed line), $s = 5$ μm and $\beta = 1 - 10^{-7}$; (a) w_y, (b) w_z.

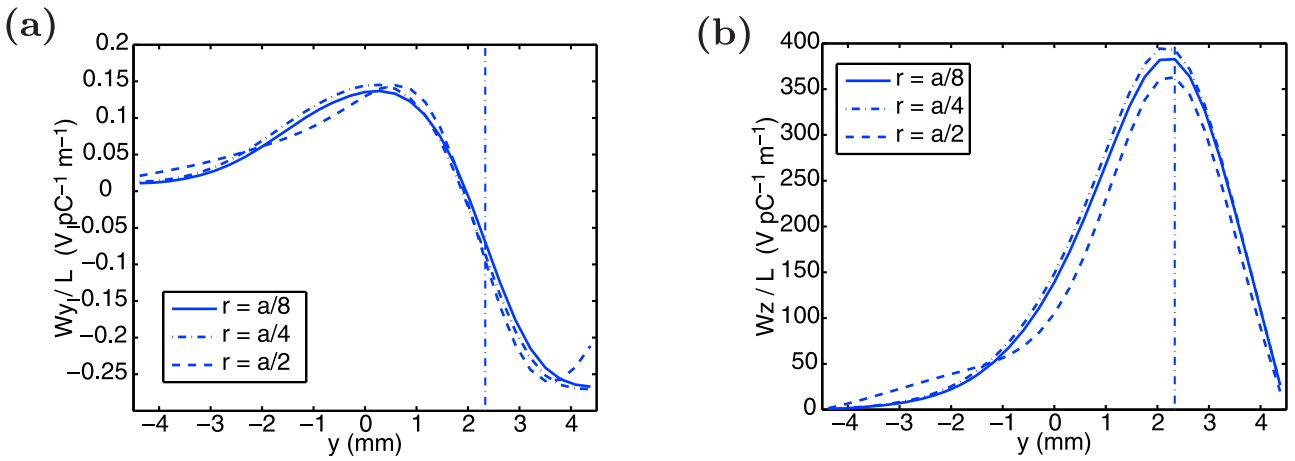

Figure 7. Dependence of the δ-function wake potential on the transverse position of a trailing charge along the y-axis for cross-shaped waveguides. The leading charge is located at the point $(x, y) = (0, 2.3)$ mm (vertical dashed line), $s = 5$ μm and $\beta = 1 - 10^{-6}$; (a) w_y, (b) w_z.

compared for several waveguides, which have different cross-sections. A total of four waveguide geometries are considered. In order to obtain comparable structures, the dimensions of the guides are such that the cut-off frequencies of the two first propagating modes are close enough to that of the original beampipe. In Figure 9 there is a picture of the different geometries analyzed, whose dimensions and cut-off frequencies are related in Table 1. Note that in most of the geometries the cut-off frequencies cannot be tuned independently, so the achieved results are not so close for the second mode.

[20] Next, the wakefield of a point charge is analyzed for the proposed waveguides. The potentials have been computed using 1800 TM-modal vectors, previously obtained by a BI-RME simulation tool. The source charge moves along the z-direction at the center of the waveguides. In Figures 10, 11, and 12, the wake potential is evaluated on the cross axes for several velocities. Only the positive semi-axes are considered because of symmetry. Despite results are similar for all the geometries, some conclusions can be extracted from these plots. The lengthwise force induced on a trailing charge is smaller in rounded-corner rectangular waveguides, whereas the response is worse in a circular waveguide; the same happens for w_x, but it is not the case for w_y. The symmetry of the circular waveguide E produces equal forces in magnitude along the transverse axes here considered. In the A waveguide, two straight cuts are introduced across the y-axis. These two cuts have the effect of increasing w_y with respect to the w_x. It is also worthwhile to mention that the wakefields produced in the waveguides A and D are very close. Finally, the dependence of the wake potential on the velocity of the particles is shown in Figure 13.

4. Conclusions

[21] The calculation of the wakefields is a primary task in the evaluation of the suitability of a beampipe. In this sense, the use of δ-function wake potentials is a good strategy for predicting the response of a waveguide to real bunches of particles. We have presented a method for the calculation of the wake potential for point charges in uniform waveguides with arbitrarily shaped cross-section. An expression for the wake potentials as a function of the vector modal functions of the waveguide has been proposed. The method consists of deriving the electromagnetic fields radiated by a point charge through the three-dimensional dyadic Green's functions of the waveguide; the wake potential is further extracted from the time domain expression of the fields. A few examples are included in the article to show the capabilities of the presented method. Modal analysis of the geometries in the examples are accomplished by a BI-RME based tool. The flexibility and efficiency of the BI-RME method makes possible an accurate computation of the modes of arbitrary waveguides. In the examples, the influence of the trajectory

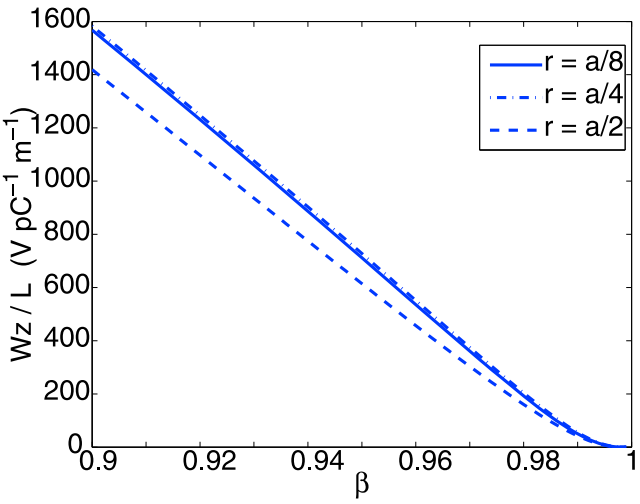

Figure 8. Dependence of w_z on the velocity of the charges. Both charges travel on the center of the waveguide and $s = 1$ mm.

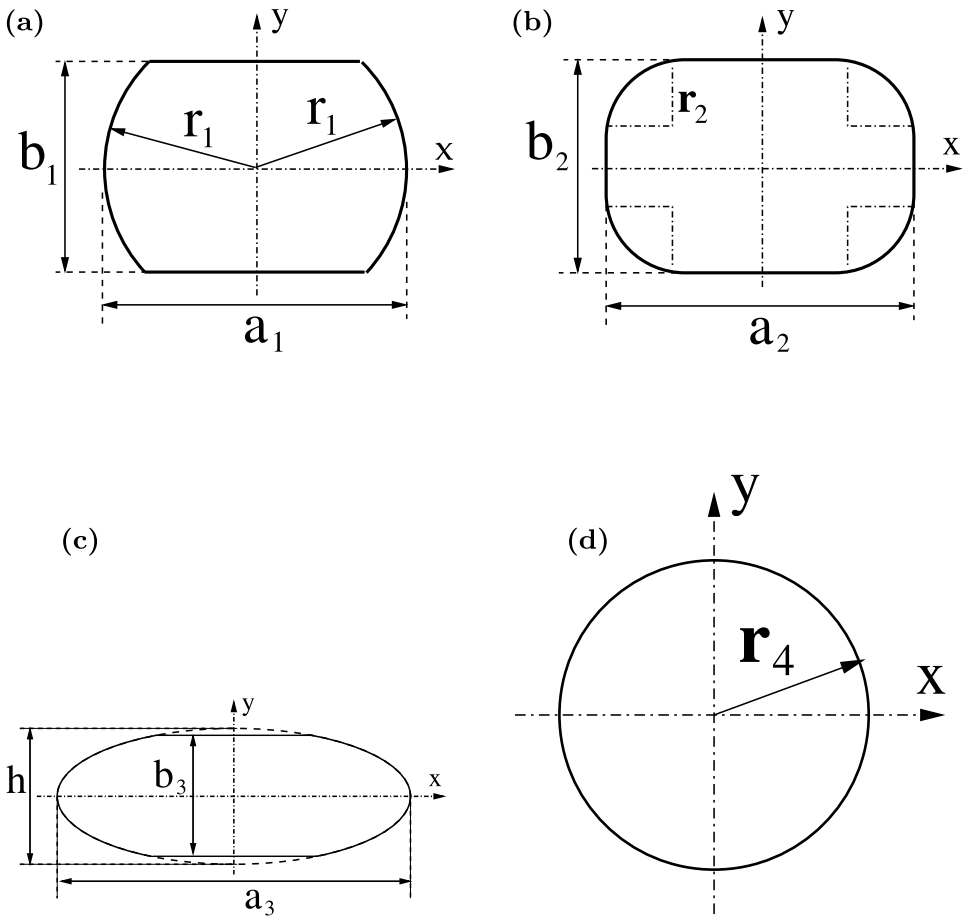

Figure 9. Cross-section of the waveguides studied in section 3.2: (a) LHC beampipe, (b) rounded-corner rectangular waveguide, (c) LHC beampipe modified with elliptical sidewalls, and (d) circular waveguide.

and the velocity of charges on the wakefields is compared for different geometries, emphasizing the rounded-corner effect of the waveguides used in particle accelerator structures.

Appendix A: Frequency to Time Domain Transformation of Field Expressions

[22] The calculation of the time domain field expressions (11) is outlined in the present appendix. For this purpose, the inverse Fourier transform (7) will be applied to the frequency domain field equations (10). The transformation of the electric field transverse component is tackled next. From (10a) one can write:

$$\vec{\mathcal{E}}_t(\mathbf{r},t) = \frac{q}{v\varepsilon_0}\sum_m k_{t_m}^2 \mathbf{e}_m^{TM}(\mathbf{r}_t)\Phi_m^{TM}(\mathbf{r}_0)\int_{-\infty}^{+\infty}\frac{e^{-i\omega z/v}e^{i\omega t}}{\left(\frac{\omega}{v\gamma}\right)^2 + k_{t_m}^2}d\omega \quad \text{(A1)}$$

The integral in (A1) can be rewritten as:

$$(v\gamma)^2\int_{-\infty}^{+\infty}\frac{e^{-i\omega z/v}}{\omega^2 + (k_{t_m}v\gamma)^2}e^{i\omega t}d\omega \quad \text{(A2)}$$

In order to solve this equation, the following Fourier pair has to be used:

$$\frac{1}{2\pi}\int_{-\infty}^{+\infty}\frac{1}{\omega^2 + A^2}e^{i\omega t}d\omega = \frac{1}{2A}e^{-A|t|} \quad \text{(A3)}$$

The application of this last relation and the shifting property of Fourier transform into (A2) leads to the equation (11a). The procedure followed for the calculation of the transverse component of the magnetic field is completely similar to the previous one.

Table 1. Waveguides Used in Section 3.2 and Cut-Off Frequencies for the First Two Modes[a]

WG	Figure	Dimensions	f_{c_1}	f_{c_2}
A	9a	$a_1 = 44$, $b_1 = 36$, $r_1 = 22$	3.84	4.49
B	9b	$a_2 = 39$, $b_2 = 34$, $r_2 = 3$	3.86	4.43
C	9b	$a_2 = 44$, $b_2 = 36$, $b_2 = 15.3$	3.80	4.56
D	9c	$a_3 = 46$, $b_3 = 32$, $h = 34$	3.82	5.22
E	9d	$r_4 = 22$	3.99	5.21

[a]Dimensions are expressed in mm and cut-off frequencies in GHz.

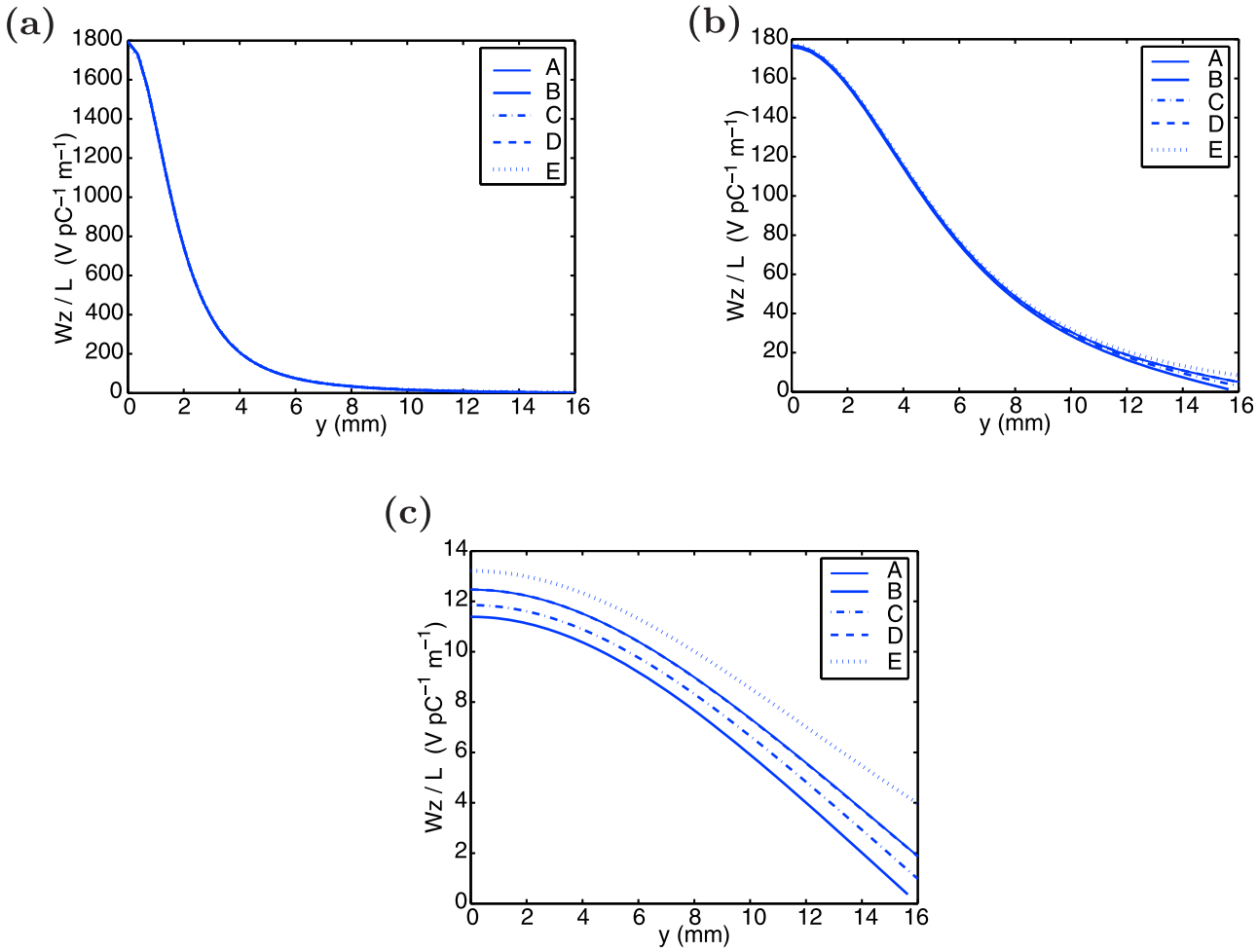

Figure 10. The w_z/L on the positive y-semiaxis for different particle velocities. The source charge is located at the center of the waveguide, $s = 10$ μm; (a) $\beta = 1 - 10^{-5}$, (b) $\beta = 1 - 10^{-6}$, (c) $\beta = 1 - 10^{-7}$.

[23] On the other hand, the next integral must be solved for the calculation of the longitudinal field (10b):

$$\int_{-\infty}^{+\infty} \frac{1}{i\omega} \cdot \frac{e^{-i\omega z/v}}{\left(\frac{\omega}{v\gamma}\right)^2 + k_{t_m}^2} e^{i\omega t} d\omega \tag{A4}$$

Note that this integral is like (A2) but multiplied by the factor $\frac{1}{i\omega}$. In order to solve it, the integration property of Fourier transform has to be applied to the Fourier pair (A3):

$$\frac{1}{2\pi}\int_{-\infty}^{+\infty} \frac{1}{i\omega} \cdot \frac{1}{\omega^2 + A^2} e^{i\omega t} d\omega = \int_{-\infty}^{t} \frac{1}{2A} e^{-A|\tau|} d\tau = -\frac{1}{2A^2} u(t) e^{-A|t|} \tag{A5}$$

Finally, the shifting term z/v is applied, thus obtaining the field expression (11b).

Appendix B: Ultrarelativistic Case Fields Derivation

[24] The derivation of the expression (12) for the time domain fields of the ultrarelativistic case is shown in this appendix. The analysis starts on the transverse component of the electric field. The ultrarelativistic limit of (11a) is:

$$\lim_{v \to c^-} \vec{\mathcal{E}}_t(\mathbf{r}, t) = \frac{q}{2\varepsilon_0} \sum_m k_{t_m} \mathbf{e}_m^{TM}(\mathbf{r}_t) \Phi_m^{TM}(\mathbf{r}_0). \tag{B1}$$

$$\lim_{v \to c^-} \gamma e^{-k_{t_m}\gamma|vt - z|} \tag{B2}$$

Knowing $\lim_{v \to c^-} \gamma \to \infty$, the previous expression constitutes an indeterminate form except for zero value of the exponent ($ct = z$). L'Hopital's rule applies when the exponent is different from zero, obtaining:

$$\lim_{v \to c^-} \gamma e^{-k_{t_m}\gamma|vt - z|}\big|_{vt \neq z} = 0 \tag{B3}$$

On the other hand, this limit diverges when the exponent is zero:

$$\lim_{v \to c^-} \gamma e^{-k_{t_m}\gamma|vt - z|}\big|_{vt = z} = \infty \tag{B4}$$

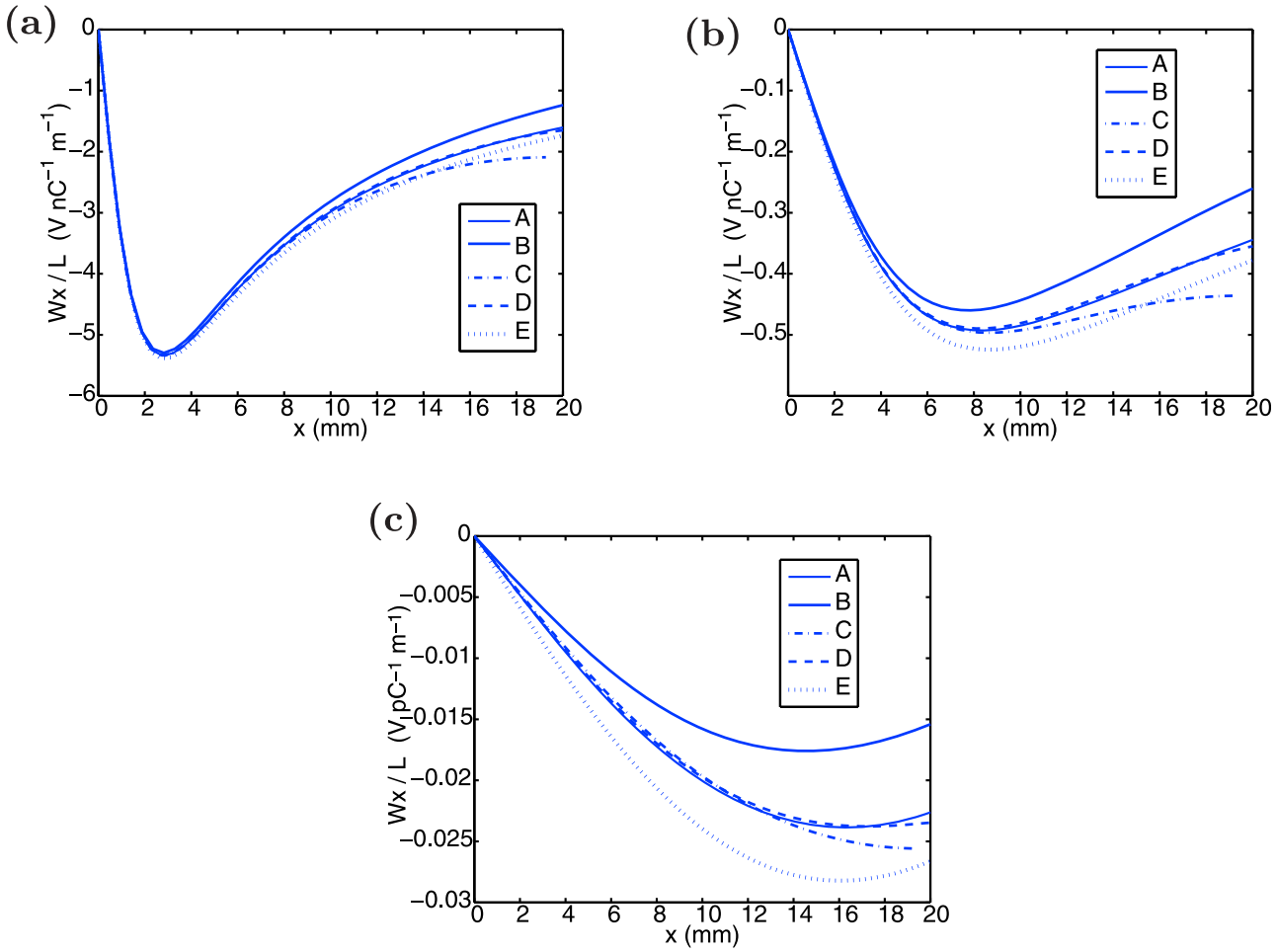

Figure 11. The w_x/L on the positive x-semiaxis for different particle velocities. The source charge is located at the center of the waveguide, $s = 10$ μm; (a) $\beta = 1 - 10^{-5}$, (b) $\beta = 1 - 10^{-6}$, (c) $\beta = 1 - 10^{-7}$.

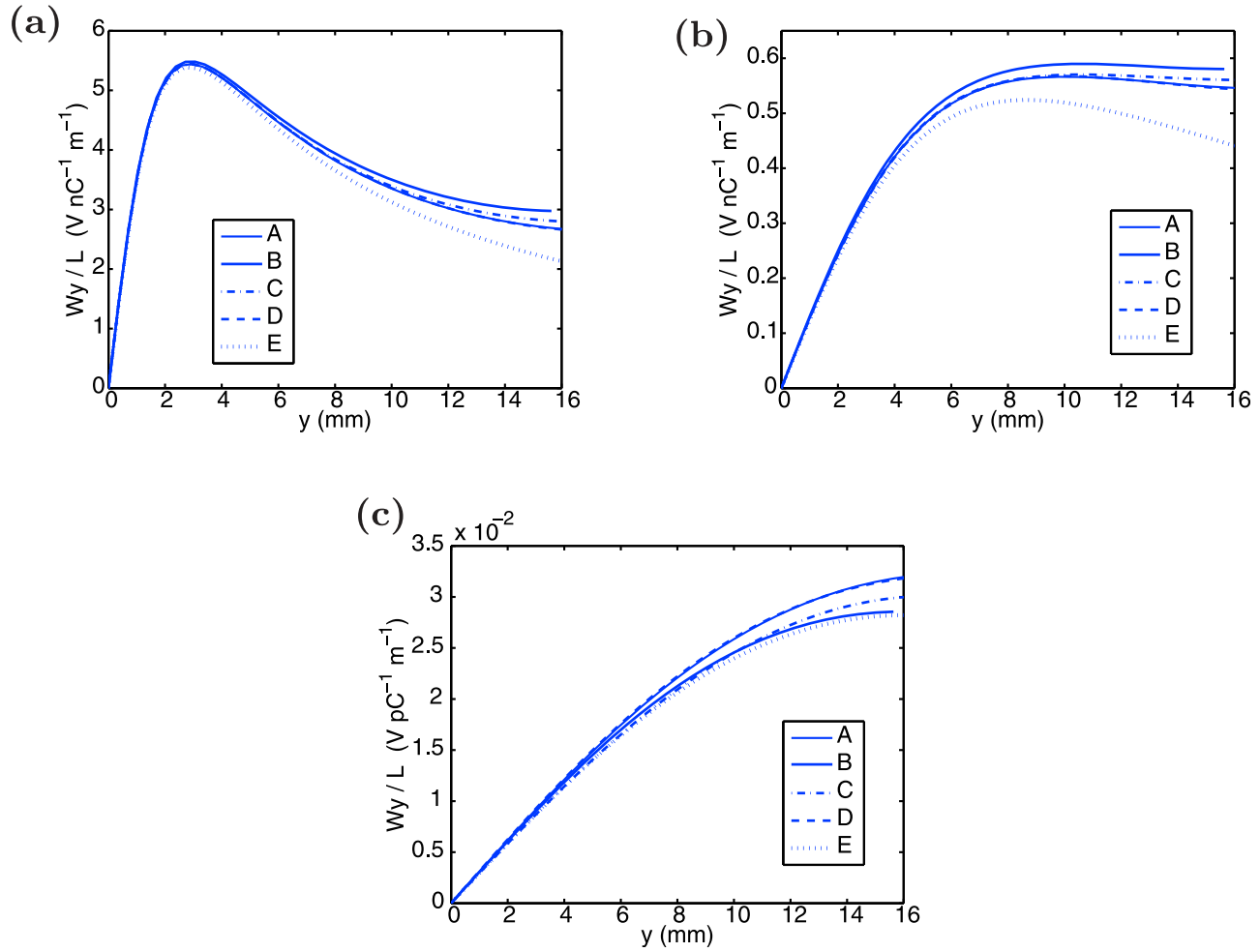

Figure 12. The w_y/L on the positive y-semiaxis for different particle velocities. The source charge is located at the center of the waveguide, $s = 10$ μm; (a) $\beta = 1 - 10^{-5}$, (b) $\beta = 1 - 10^{-6}$, (c) $\beta = 1 - 10^{-7}$.

These two results can be combined by means of the Dirac-delta function, thus leading to the expression

$$\lim_{v\to c^-} \vec{\mathcal{E}}_t(\mathbf{r},t) = \frac{q}{2\varepsilon_0}\sum_m k_{t_m}\mathbf{e}_m^{TM}(\mathbf{r}_t)\Phi_m^{TM}(\mathbf{r}_0)\delta(ct-z) \tag{B5}$$

which is equivalent to (12a). A similar analysis can be followed for the transverse magnetic field (12c). For the analysis of the longitudinal electric field, the ultrarelativistic limit is applied to (11b):

$$\lim_{v\to c^-} \mathcal{E}_z(\mathbf{r},t) = -\frac{q}{2\varepsilon_0}\sum_m k_{t_m}^2\Phi_m^{TM}(\mathbf{r}_t)\Phi_m^{TM}(\mathbf{r}_0). \tag{B6}$$

$$\lim_{v\to c^-} u\left(t-\frac{z}{v}\right)e^{-k_{t_m}\gamma|vt-z|} \tag{B7}$$

The resulting limit can be analyzed for zero and different from zero values of the exponent:

$$\lim_{v\to c^-} u\left(t-\frac{z}{v}\right)e^{-k_{t_m}\gamma|vt-z|}\Big|_{vt\neq z} = 0 \tag{B8}$$

$$\lim_{v\to c^-} u\left(t-\frac{z}{v}\right)e^{-k_{t_m}\gamma|vt-z|}\Big|_{vt=z} = u(0) = 0 \tag{B9}$$

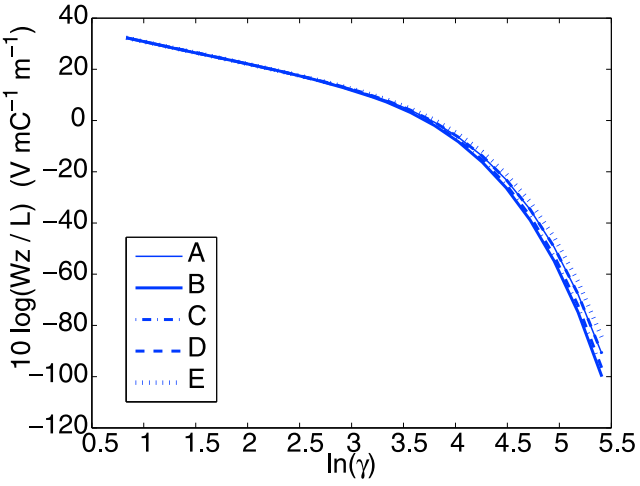

Figure 13. Dependence of w_z on the velocity. The leading charge travels along the center of the waveguide; $s = 1$ mm. A logarithmic scale has been chosen to emphasize differences at high velocities.

This time, the limit is zero in both cases, and hence the null expression for the longitudinal field (12b), as predicted by Lorentz.

Appendix C: Wake Potentials Derivation

[25] The derivation of the δ-function wake potential (14) from the definition given in (13) is detailed in the present appendix. First of all, the time domain field expression (11) is used in (13):

$$\mathbf{w}_t(\mathbf{r},\mathbf{r}',s)=\frac{\gamma}{2\varepsilon_0}\sum_m k_{t_m}\mathbf{e}_m^{TM}(\mathbf{r}_t)\Phi_m^{TM}(\mathbf{r}_0)I_m^{(1)} + \frac{\nu^2\gamma\mu_0}{2}\sum_m k_{t_m}\Phi_m^{TM}(\mathbf{r}_0)\left(\hat{z}\times\mathbf{h}_m^{TM}(\mathbf{r}_t)\right)I_m^{(1)} \quad \text{(C1a)}$$

$$w_z(\mathbf{r},\mathbf{r}',s)=\frac{1}{2\varepsilon_0}\sum_m k_{t_m}^2\Phi_m^{TM}(\mathbf{r}_t)\Phi_m^{TM}(\mathbf{r}_0)I_m^{(2)} \quad \text{(C1b)}$$

where the following integrals have been introduced, obtaining:

$$I_m^{(1)}\equiv\int_0^L e^{-k_{t_m}\gamma|vt-z|}\Big|_{t=\frac{z+s}{v}}dz=Le^{-k_{t_m}\gamma|s|} \quad \text{(C2a)}$$

$$I_m^{(2)}\equiv\int_0^L u\left(t-\frac{z}{v}\right)e^{-k_{t_m}\gamma|vt-z|}\Big|_{t=\frac{z+s}{v}}dz=Lu\left(\frac{s}{v}\right)e^{-k_{t_m}\gamma|s|} \quad \text{(C2b)}$$

On the other hand, knowing that $\hat{z}\times\mathbf{h}_m=-\mathbf{e}_m$ and $\nu^2\gamma\mu_0/2=\gamma/(2\varepsilon_0)-1/(2\gamma\varepsilon_0)$, the transverse component (C1a) can be simplified as

$$\mathbf{w}_t(\mathbf{r},\mathbf{r}',s)=\frac{1}{2\gamma\varepsilon_0}\sum_m k_{t_m}\mathbf{e}_m^{TM}(\mathbf{r}_t)\Phi_m^{TM}(\mathbf{r}_0)I_m^{(1)} \quad \text{(C3)}$$

Finally, assuming positive distance s, the previous expressions yield the equation (13).

[26] **Acknowledgments.** The authors would like to thank ESA/ESTEC for having cofunded this research activity through the Network Partnering Initiative program and through the project "Multipactor Analysis in Planar Transmission Lines" (contract 20841/08/NL/GLC). We also are grateful to the Spanish government and the local Council of Murcia for their support through the projects CICYT Ref. TEC2010-21520-C04-04 and SENECA Ref. 08833/PI/08, respectively.

References

Álvarez Melcón, A., and J. R. Mosig (1999), A novel procedure for the use of the Shanks' transformation in the efficient evaluation of the boxed Green's functions, in *ISRAMT'99 International Symposium on Recent Advances in Microwave Technology*, pp. 605–608, Univ. de Malaga, Malaga, Spain.

Álvarez Melcón, A., and J. R. Mosig (2000), Two techniques for the efficient numerical calculation of the Green's functions for planar shielded circuits and antennas, *IEEE Trans. Microwave Theory Tech.*, *48*(9), 1492–1504.

Bane, K. L. F., P. B. Wilson, and T. Weiland (1985), Wake fields and wake field acceleration, *AIP Conf. Proc.*, *127*, 875–928.

Bozzi, M., L. Perregrini, A. Álvarez Melcón, M. Guglielmi, and G. Conciauro (2001), MoM-BIRME analysis of boxed MMICs with arbitrarily shaped metalizations, *IEEE Trans. Microwave Theory Tech.*, *49*(12), 2227–2234.

Burov, A., and V. Danilov (1999), Suppression of transverse bunch instabilities by asymmetries in the chamber geometry, *Phys. Rev. Lett.*, *82*(11), 2286–2289, doi:10.1103/PhysRevLett.82.2286.

Cogollos, S., S. Marini, V. E. Boria, P. Soto, A. Vidal, H. Esteban, J. V. Morro, and B. Gimeno (2003), Efficient modal analysis of arbitrarily shaped waveguides composed of linear, circular, and elliptical arcs using the BI-RME method, *IEEE Trans. Microwave Theory Tech.*, *51*(12), 2378–2390.

Collin, R. E. (1991), *Field Theory of Guided Waves*, IEEE Press, Piscataway, N. J.

Conciauro, G., M. Bressan, and C. Zuffada (1984), Waveguide modes via an integral equation leading to a linear matrix eigenvalue problem, *IEEE Trans. Microwave Theory Tech.*, *32*(11), 1495–1504.

Conciauro, G., M. Guglielmi, and R. Sorrentino (2000), *Advanced Modal Analysis - CAD Techniques for Waveguide Components and Filters*, John Wiley, New York.

Danilov, V. (2000), Extended definitions of wake fields and their influence on beam dynamics, *Phys. Rev. Special Topics - Accel. Beams*, *3*, 1–5, doi:10.1103/PhysRevSTAB.3.014201.

Deshpande, M. D. (1997), Analysis of discontinuities in a rectangular waveguide using dyadic Green's function approach in conjuntion with Method of Moments, *Rep. NASA-CR-201692*, Langley Res. Cent., NASA, Hampton, Va.

Felsen, L. B., and N. Marcuvitz (1994), *Radiation and Scattering of Waves*, IEEE Press, Piscataway, N. J.

Figueroa, H., W. Gai, R. Konecny, J. Norem, A. Ruggiero, P. Schoessow, and J. Simpson (1988), Direct measurement of beam-induced fields in accelerating structures, *Phys. Rev. Lett.*, *60*, 2144–2147, doi:10.1103/PhysRevLett.60.2144.

Gai, W., A. Kanareykin, A. L. Kustov, and J. Simpson (1997), Numerical simulations of intense charged-particle beam propagation in a dielectric wake-field accelerator, *Phys. Rev. E*, *55*, 3481–3488, doi:10.1103/PhysRevE.55.3481.

Gluckstern, R., J. van Zeijts, and B. Zotter (1993), Coupling impedance of beam pipes of general cross section, *Phys. Rev. E*, *74*(1), 656–663.

Hanson, G. W., and A. B. Yakovlev (2002), *Operator Theory for Electromagnetics*, Springer, New York.

Hess, M., C. S. Park, and D. Bolton (2007), Green's function based space-charge field solver for electron source simulations, *Phys. Rev. Spec. Top. Accel. Beams*, *10*(5), 054201, doi:10.1103/PhysRevSTAB.10.054201.

Iriso-Ariz, U., F. Caspers, and A. Mostacci (2003), Evaluation of the horizontal to vertical transverse impedance ratio for LHC beam screen using a 2D electrostatic code, in *20th IEEE Particle Accelerator Conference, Portland, OR, USA, 12–16 May 2003*, pp. 3479–3483, IEEE Press, Piscataway, N. J.

Jackson, J. D. (1999), *Classical Electrodynamics*, John Wiley, New York.

Jing, C., W. Liu, L. Xiao, W. Gai, and P. Schoessow (2003), Dipole-mode wakefields in dielectric-loaded rectangular waveguide accelerating structures, *Phys. Rev. E*, *68*(1), 016502, doi:10.1103/PhysRevE.68.016502.

Kim, S. H., K. W. Chen, and J. S. Yang (1990), Modal analysis of wake fields and its application to elliptical pill-box cavity with finite aperture, *J. Appl. Phys.*, *68*(10), 4942–4951.

Lutman, A., R. Vescovo, and P. Craievich (2008), Electromagnetic field and short-range wake function in a beam pipe of elliptical cross section, *Phys. Rev. Spec. Top. Accel. Beams*, *11*(7), 074401, doi:10.1103/PhysRevSTAB.11.074401.

Ng, K.-Y. (1990), Wake fields in a dielectric-lined waveguide, *Phys. Rev. D*, *42*(5), 1819–-1828, doi:10.1103/PhysRevD.42.1819.

Palumbo, L., V. Vaccaro, and G. Wustefeld (1984), Coupling impedance in circular accelerators, circular beam, elliptic chamber, *IEEE Trans. Nucl. Sci.*, *31*(4), 1011–1020.

Panofsky, W. K. H., and W. A. Wenzel (1956), Some considerations concerning the transverse deflection of charged particles in radio-frequency fields, *Rev. Sci. Instrum.*, *27*(11), 967.

Rahmat-Samii, Y. (1975), On the question of computation of the dyadic Green's function at the source region in waveguides and cavities, *IEEE Trans. Microwave Theory Tech.*, *23*(9), 762–765.

Rosing, M., and W. Gai (1990), Longitudinal- and transverse-wake-field effects in dielectric structures, *Phys. Rev. D*, *42*(5), 1829–1834, doi:10.1103/PhysRevD.42.1829.

Rumolo, G., F. Ruggiero, and F. Zimmermann (2001), Simulation of the electron-cloud build up and its consequences on heat load, beam stability, and diagnostics, *Phys. Rev. Spec. Top. Accel. Beams*, *4*(1), 012801, doi:10.1103/PhysRevSTAB.4.012801.

Salah, W. (2004), Analytical and numerical investigations of the evolution of wake fields of accelerated electron beams encountering cavity discontinuities in laser-driven RF-free electron laser photoinjector, *Nucl. Instrum. Methods Phys. Res., Sect. A*, *533*, 248–257, doi:10.1016/j.nima.2004.05.129.

Salah, W., and J.-M. Dolique (1999), Wake field of electron beam accelerated in a RF-gun of free electron laser elsa, *Nucl. Instrum. Methods Phys. Res., Sect. A*, *431*(1–2), 27–37.

Stupakov, G., K. L. F. Bane, and I. Zagorodnov (2007), Optical approximation in the theory of geometric impedance, *Phys. Rev. Spec. Top. Accel. Beams*, *10*(5), 054401, doi:10.1103/PhysRevSTAB.10.054401.

Tai, C.-T. (1993), *Dyadic Green's Functions in Electromagnetic Theory*, IEEE Press, Piscataway, N. J.

Wang, J. J. H. (1978), Analysis of three-dimensional arbitrarily shaped dielectric or biological body inside a rectangular waveguide, *IEEE Trans. Microwave Theory Tech.*, *26*(7), 457–462.

Wangler, T. P. (2008), *RF Linear Accelerators*, John Wiley, New York.

Xiao, L., W. Gai, and X. Sun (2001), Field analysis of a dielectric-loaded rectangular waveguide accelerating structure, *Phys. Rev. E*, *65*(1), 016505, doi:10.1103/PhysRevE.65.016505.

Yokoya, K. (1993a), Resistive wall impedance of beam pipes of general cross section, *Particle Accel.*, *41*, 221–248.

Yokoya, K. (1993b), Resistive wall impedance of beam pipes of general cross section, *KEK Prepr.*, *74*, 93–196.

Zagorodnov, I. (2006), Indirect methods for wake potential integration, *Phys. Rev. Spec. Top. Accel. Beams*, *9*(10), 102002, doi:10.1103/PhysRevSTAB.9.102002.

Zimmermann, F. (1997), A simulation study of electron-cloud instability and beam-induced multipacting in the LHC, *CERN LHC Proj. Rep. 95*, Eur. Org. for Nucl. Res., Geneva, Switzerland.

Zotter, B. W., and S. A. Kheifets (1998), *Impedances and Wakes in High-Energy Particle Accelerators*, World Sci, Singapore.